JACS
JOURNAL OF THE AMERICAN CHEMICAL SOCIETY
Communication
pubs.acs.org/JACS

^{15}N Heteronuclear Chemical Exchange Saturation Transfer MRI

Haifeng Zeng,*[,†,‡] Jiadi Xu,[†,‡] Nirbhay N. Yadav,[†,‡] Michael T. McMahon,[†,‡] Bradley Harden,[§] Dominique Frueh,[§] and Peter C. M. van Zijl*[,†,‡]

[†]Russell H. Morgan Department of Radiology and Radiological Science and [§]Department of Biophysics and Biophysical Chemistry, Johns Hopkins University School of Medicine, Baltimore, Maryland 21205, United States

[‡]F. M. Kirby Research Center for Functional Brain Imaging, Kennedy Krieger Research Institute, Baltimore, Maryland 21205, United States

Supporting Information

ABSTRACT: A two-step heteronuclear enhancement approach was combined with chemical exchange saturation transfer (CEST) to magnify ^{15}N MRI signal of molecules through indirect detection via water protons. Previous CEST studies have been limited to radiofrequency (rf) saturation transfer or excitation transfer employing protons. Here, the signal of ^{15}N is detected indirectly through the water signal by first inverting selectively protons that are scalar-coupled to ^{15}N in the urea molecule, followed by chemical exchange of the amide proton to bulk water. In addition to providing a small sensitivity enhancement, this approach can be used to monitor the exchange rates and thus the pH sensitivity of the participating ^{15}N-bound protons.

Magnetic resonance imaging (MRI) has become an indispensable noninvasive diagnostic tool to image soft tissue. In addition to anatomical images, MRI can also provide functional information such as motion, flow, perfusion, and diffusion. Traditional MRI exclusively relies on water protons and hence only reports on these water molecules. Heteronuclei such as ^{15}N, ^{31}P, and ^{13}C are promising reporters of biomarkers that could be used in molecular imaging.[1,2] However, their low gyromagnetic ratio and low molecular concentration results in dramatically reduced sensitivity. Recently, chemical exchange saturation transfer (CEST)[3−6] has shown great potential in detecting low-concentration metabolites and proteins. In CEST, the magnetization of exchangeable solute protons is labeled by spin manipulations (e.g., saturation) and transferred to water via exchange. Rapid exchange allows for multiple carry-overs, and labeling of solute spin magnetization accumulates in the water pool thereby increasing sensitivity. The CEST technique has been successfully applied to image several physiologically important molecules such as proteins,[7−9] creatine,[10,11] glucose,[12,13] glycogen,[14] and glycosaminoglycans.[15] The exchange rates of these exchangeable protons often depend on pH, and CEST has been used to image pH changes during ischemia.[7,16,17] In high-resolution NMR, CEST has been used to study low populated invisible states of proteins.[18,19]

Although traditionally, CEST is obtained via RF saturation of exchangeable proton spins, in principle, any perturbation of the exchangeable proton spin magnetization can be observed in the water pool, including one propagated from nonexchangeable protons to exchangeable protons via intramolecular relayed NOEs.[4,20,21] Here, we expand CEST methods to perturbations involving heteronuclei. We focus on the ^{15}N nucleus because nitrogen is abundant in proteins and because the amide protons that are bound to ^{15}N can exchange with water at various rates, depending on their location in proteins and on physiological conditions such as pH.[7−9,22,23] To demonstrate the principle, we use ^{15}N-labeled urea and evaluate the influence of exchange rate (k) by varying pH.

To obtain CEST effects of ^{15}N-labeled molecules, we used BIRD building blocks[24] in a pulse sequence derived from the frequency-labeled exchange (FLEX) principle.[25,26] ^{15}N discrimination is obtained via alternate application of a ^{15}N refocusing pulse at the center of a proton spin−echo of length $2\tau = 1/J_{NH}$ (Figure 1), where J_{NH} is the ^{15}N−^{1}H scalar coupling constant.

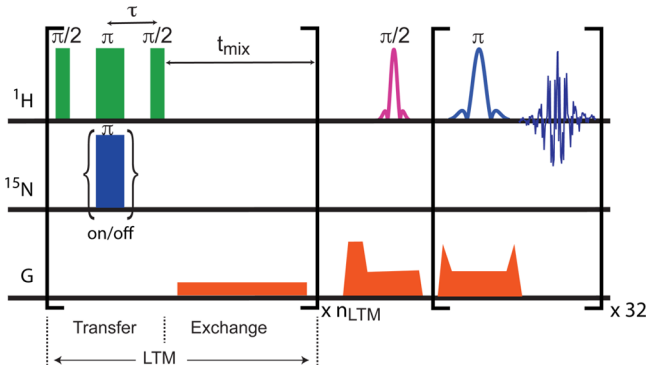

Figure 1. Pulse sequence for acquisition of MRI images reporting on ^{15}N. Flip angles are indicated above the pulses. The phases of the hard pulses in a LTM are x, $-x$, x, respectively. $2\tau \sim 1/J_{NH}$. G indicates field gradients. The preparation time contains n_{LTM} LTMs.

This alternation engages and disengages evolution under J_{NH} scalar coupling, resulting in a spin magnetization discrimination specific to protons coupled to ^{15}N. Next, magnetization of exchangeable protons is transferred to water during a period t_{mix}. To enhance the signal, the BIRD-t_{mix} label transfer module (LTM) is repeated multiple times (n_{LTM}) in a manner that closely resembles the FLEX experiment, but does not include

Received: July 13, 2016
Published: August 22, 2016

DOI: 10.1021/jacs.6b06421
J. Am. Chem. Soc. 2016, 138, 11136−11139

the chemical shift encoding under t_1 evolution used in FLEX. The efficiency of the heteronuclear magnetization transfer (see Supporting Information (SI)) depends on J_{NH} (−89 Hz for urea), the exchange rate of urea protons (k), and the transverse and longitudinal relaxation rates of water and urea protons. To detect a heteronuclear CEST effect, k has to be in a proper range. When k is too large, the magnetization will decay too much during the BIRD period. However, when k is too small, negligible CEST enhancement will be achieved due to lack of transfer of labeled protons during t_{mix}.

Urea ($^{15}N_2$, >98%) was purchased from Cambridge Isotopes and used without further purification. Solutions were freshly prepared in phosphate-buffered saline (PBS), titrated to desired pH values, and transferred to 5 mm NMR tubes. The range of pH values corresponded to exchange rates (k) of amide protons that include measurable, too fast, and too slow exchange for our transfer experiment. Note that k is minimal close to neutral pH and high under both acidic and basic conditions. These rates were measured using a saturation recovery scheme and assuming that $R_1 = 1/T_1$ is negligible (Table 1).

Table 1. pH and Exchange Rates (k) at 21 °C

pH	4.1	4.5	5.0	5.4	5.6	5.9	6.2
k (Hz)	222	141	34.9	21.5	11.8	7.3	3.5

MRI experiments were performed on a vertical bore 17.6 T (750 MHz) scanner (Bruker, Ettlingen, Germany) at 21 °C. A broadband inverse (BBI) 5 mm probe was used for NMR experiments and a 25 mm heteronuclear volume coil ($^1H/^{15}N$) for MRI. Images were acquired using a RARE sequence with TR/TE = 10 s/8.0 ms, RARE factor 32, slice thickness 4 mm, matrix size 128 × 128, and FOV 2.0 × 2.0 cm^2. The pulses on the ^1H channel were applied on resonance with water, those on ^{15}N on resonance with ^{15}N of urea. The ^1H 90° and 180° pulse widths were 0.11 and 0.22 ms, respectively; the ^{15}N 180° pulse width was 0.22 ms. This ^{15}N pulse was calibrated by varying the pulse power and searching for the maximum signal difference from a counterpart image without ^{15}N pulses. We also acquired a series of ^{15}N spectra using a fixed pulse power while varying the pulse length with the 180° pulse length determined from the first null point. The results of these two experiments matched. The LTM module was repeated multiple times without phase cycling. A 1.5 G/cm z gradient was applied during t_{mix} to crush unwanted water magnetization that may cause radiation damping.

Using the experimental setup mentioned above, two images were acquired (Figure 2), one for reference without pulses on ^{15}N channel (I_{off}), the other with ^{15}N 180° pulses (I_{on}). The signal difference between these two images is due to the ^{15}N-based CEST effects. The "on" and "off" images show equivalent in-plane B0 inhomogeneity over the sample, which consisted of a group of sample tubes bound together. The signal intensities were not sensitive to any B1 field inhomogeneity in the ^{15}N pulse. This can be seen from the difference data, which are homogeneous. The normalized difference signal, I_{diff}, is defined as

$$I_{diff} = (I_{off} - I_{on})/I_{off} \times 100\% \quad (1)$$

In order to maximize the CEST difference signal for all pH values, the three parameters τ, t_{mix}, and n_{LTM} were optimized from initial values of 4.5 ms, 100 ms, and 24 using this phantom (Figure 3). In each optimization, the other two parameters were held constant as described.

Similar to proton-based CEST, heteronuclear CEST in principle benefits from larger exchange rates (k). However, during the BIRD sequence, chemical exchange competes with J coupling. Efficient coherence transfer requires that $J > k$. For

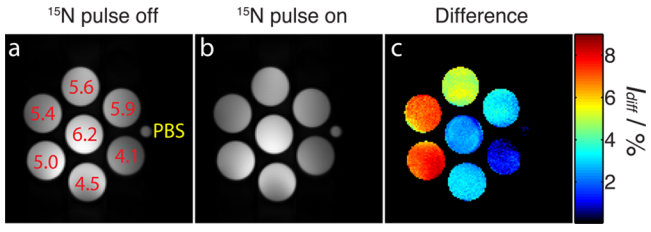

Figure 2. Images acquired with τ = 4.5 ms, t_{mix} = 100 ms and n_{LTM} = 24. ^{15}N pulse (a) off and (b) on and (c) normalized difference (eq 1). The phantom contained 7 samples of 250 mM ^{15}N-labeled urea in PBS and a capillary of PBS. The pH values are shown in (a).

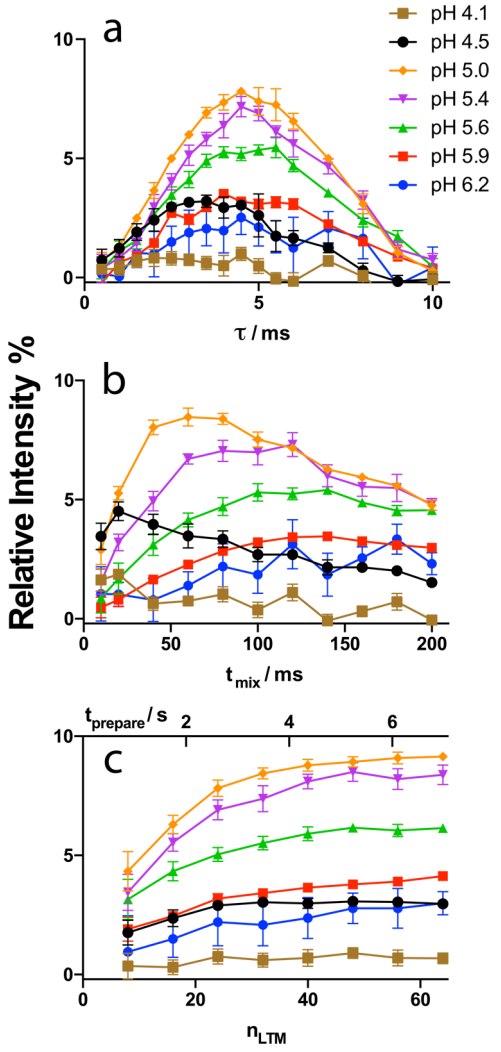

Figure 3. Optimization of the parameters (a) τ, (b) t_{mix}, and (c) n_{LTM} for heteronuclear CEST images of 250 mM ^{15}N-labeled urea. Intensities are from eq 1, namely percentage of water signal of the image without ^{15}N pulses on (I_{off}). Each LTM is about 109 ms. The length of the preparation time as a function of n_{LTM} is shown on top of (c). Error bars are the standard deviation of 8 experiments.

DOI: 10.1021/jacs.6b06421
J. Am. Chem. Soc. 2016, 138, 11136−11139

^{15}N in urea, a pH of 5.0 with an exchange rate (k) of 35 Hz was found to be the condition for maximum signal difference (Figure 3a). At pH 4.1 (k = 222 Hz), almost no CEST signal was observed. As pH increased above 5.0, k-values decreased, and CEST effects gradually diminished. For τ, a value $1/2J_{NH}$ = 5.6 ms should give the maximum transfer. However, the effect of exchange caused reduction of the optimum τ (Figure 3a). In larger molecules, faster transverse relaxation will also contribute to reducing the optimum τ.

Finally, a larger number of LTMs leads to a higher CEST signal until a plateau is reached (Figure 3c). The reason is that the contribution of each LTM to the total signal decays exponentially with a rate depending on T_1 of water during both the coherence-transfer and exchange-transfer steps[25,26] (see the formulas in the SI). Figure 3c shows that we obtain about 80% of the maximum CEST effects using 24 LTMs.

Using a steady-state approximation for the magnetization of urea protons, the CEST signal can be estimated using the following parameters: x (ratio of urea proton concentration to water proton concentration); the longitudinal and transverse relaxation rates of urea and water protons without exchange effect R_{1u}, R_{2u}, R_{1w}, R_{2w}. The signal difference for two scans is

$$I_{diff} = \frac{(A_{1w}A_{2w})^n - 1}{A_{1w}A_{2w} - 1}(1 - A_{ex})A_{1w}A_{2u} \times xM_w\left(\frac{1 - A_{1u}}{1 - A_{1u}A_{2u}} - \frac{(1 - A_{1u})\cos(2\pi J\tau)}{1 - A_{1u}A_{2u}\cdot\cos(2\pi J\tau)}\right) \quad (2)$$

in which M_w is the experimentally determined average of the water magnetization over the preparation period (see SI), $A_{1u} = e^{-(k+R_{1u})t_{mix}}$, $A_{2u} = e^{-2(k+R_{2u})\tau}$, $A_{1w} = e^{-R_{1w}t_{mix}}$, $A_{2w} = e^{-2(kx+R_{2w})\tau}$, and $A_{ex} = e^{-(1+x)kt_{mix}}$.

Using eq 2 with experimental parameters reproduced the experimental results in Figure 3 (see SI) and confirmed our discussion of the effects of τ, t_{mix}, n_{LTM}, and k on the signal intensities. Optimal conditions for studies of other systems such as proteins can be estimated with eq 2. Using J_{NH} = −92 Hz,[27] simulations show that the optimum exchange rate (k) is 30 Hz, which is quite insensitive to the values of the transverse and longitudinal relaxation rates used in the simulations. The theoretical parameters to achieve the maximum signal are τ = 5.0 ms, t_{mix} = 100 ms, which are very close to experimental observations. These values are valid when k and relaxation rates are slower than $1/J_{NH}$. For very fast exchange or slow molecular tumbling, e.g., larger proteins, the optimum duration of τ and t_{mix} will be different. To make predictions, the simple principle is that a larger coupling allows use of a higher exchange rate, leading to increased CEST effects.

To test the effects of concentration, heteronuclear CEST MRI images of samples of 1 M nonlabeled urea and 1M, 250 mM, 100 mM, and 25 mM ^{15}N-labeled urea were acquired at pH = 5.0. The data in Figure 4 show that, for this concentration of urea protons (1M) that is low relative to water protons (110M), the CEST signal was proportional to the concentration of ^{15}N-labeled urea. At higher concentrations, back exchange may reduce the CEST effect. There is no visible effect on nonlabeled urea. Using this scheme, we can thus selectively image ^{15}N-labeled samples.

Compared to imaging ^{15}N directly, this bilinear rotation decoupling chemical exchange saturation transfer scheme enhances the ^{15}N signal in two ways. First, the gyromagnetic

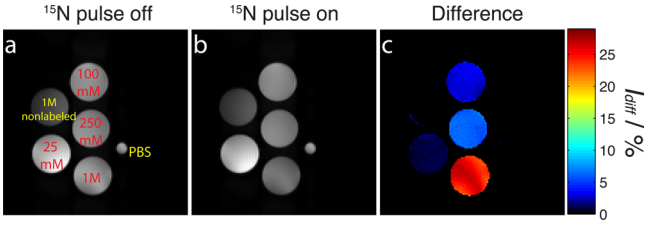

Figure 4. Image acquired with ^{15}N pulse (a) off and (b) on and (c) the difference image, using samples of 1 M, 250 mM, 100 mM, 25 mM ^{15}N-labeled urea and 1 M nonlabeled urea at pH 5.0.

ratio (γ) of ^{1}H is 10 times that of ^{15}N. By using proton excitation and detection, the sensitivity is increased by a factor $(\gamma_H/\gamma_N)^{5/2} \sim 300$. Second, CEST enhancement can be estimated from our measurements with 250 mM urea (1 M protons), where optimal parameter conditions lead to a signal difference of about 8% (Figure 3). However, this is based on eq 1, where I_{off} is done with a series of proton pulses and delay times, similar to I_{on}, and the water signal reduces for increased number of LTMs due to T_2 relaxation during 2τ in each LTM. When compared to the situation without a preparation period, the effective increase was only 4.5% of the water signal. Accounting for the number of protons in water and urea, we thus obtain a factor 5 enhancement for protons. So the total enhancement from 500 mM ^{15}N (two ^{15}N per urea) to water detection was a factor of about 1500. Despite such a large enhancement, application of this method *in vivo* may not be practical with imaging, but should be with spectroscopy. Using a typical water SNR of about 200:1 in a 1 × 1 × 1 mm^3 voxel, we should have a 1% effect for about 110 mM of a molecule with a singly labeled ^{15}N. In spectroscopy, use of a 10 × 10 × 10 mm^3 voxel would allow detection of 0.11 mM, which is a feasible concentration.

In summary, we demonstrated a model phantom experiment for MRI imaging of heteronuclear CEST transfer. Our proof of principle study showed that the method may permit selective imaging of ^{15}N-isotopically enriched molecules and simultaneously report on pH variations. For a J value of about −92 Hz, this method works best when the exchange rate (k) is around 30 Hz, which is close to the exchange rates of amide protons of proteins at physiological condition, shining light on the potential to image labeled proteins in vivo. The method may provide an alternative to hyperpolarization,[28] used in clinical application of heteronuclear MRI,[29,30] and is not contingent on specialized polarization equipment.

■ ASSOCIATED CONTENT

Supporting Information

The Supporting Information is available free of charge on the ACS Publications website at DOI: 10.1021/jacs.6b06421.

Derivation of equations for heteronuclear CEST enhancement and simulation plots (PDF)

■ AUTHOR INFORMATION

Corresponding Authors

*hzeng6@jhmi.edu

*pvanzijl@jhu.edu

Notes

The authors declare no competing financial interest.

DOI: 10.1021/jacs.6b06421
J. Am. Chem. Soc. 2016, 138, 11136−11139

■ ACKNOWLEDGMENTS

P.V.Z. thanks the National Institutes of Health (R01 EB015032) for financial support of this work.

■ REFERENCES

(1) Golman, K.; Ardenaer-Larsen, J. H.; Petersson, J. S.; Mansson, S.; Leunbach, I. *Proc. Natl. Acad. Sci. U. S. A.* **2003**, *100*, 10435.
(2) Mansson, S.; Johansson, E.; Magnusson, P.; Chai, C. M.; Hansson, G.; Petersson, J. S.; Stahlberg, F.; Golman, K. *Eur. Radiol.* **2006**, *16*, 57.
(3) Ward, K. M.; Aletras, A. H.; Balaban, R. S. *J. Magn. Reson.* **2000**, *143*, 79.
(4) van Zijl, P. C. M.; Yadav, N. N. *Magn. Reson. Med.* **2011**, *65*, 927.
(5) Liu, G.; Song, X.; Chan, K. W.; McMahon, M. T. *NMR Biomed.* **2013**, *26*, 810.
(6) Sherry, A. D.; Woods, M. *Annu. Rev. Biomed. Eng.* **2008**, *10*, 391.
(7) Zhou, J. Y.; Payen, J. F.; Wilson, D. A.; Traystman, R. J.; van Zijl, P. C. M. *Nat. Med.* **2003**, *9*, 1085.
(8) Jones, C. K.; Schlosser, M. J.; van Zijl, P. C. M.; Pomper, M. G.; Golay, X.; Zhou, J. Y. *Magn. Reson. Med.* **2006**, *56*, 585.
(9) Zhou, J. Y.; Blakeley, J. O.; Hua, J.; Kim, M.; Laterra, J.; Pomper, M. G.; van Zijl, P. C. M. *Magn. Reson. Med.* **2008**, *60*, 842.
(10) Haris, M.; Nanga, R. P. R.; Singh, A.; Cai, K.; Kogan, F.; Hariharan, H.; Reddy, R. *NMR Biomed.* **2012**, *25*, 1305.
(11) Kogan, F.; Haris, M.; Singh, A.; Cai, K. J.; Debrosse, C.; Nanga, R. P. R.; Hariharan, H.; Reddy, R. *Magn. Reson. Med.* **2014**, *71*, 164.
(12) Chan, K. W. Y.; McMahon, M. T.; Kato, Y.; Liu, G. S.; Bulte, J. W. M.; Bhujwalla, Z. M.; Artemov, D.; van Zijl, P. C. M. *Magn. Reson. Med.* **2012**, *68*, 1764.
(13) Walker-Samuel, S.; Ramasawmy, R.; Torrealdea, F.; Rega, M.; Rajkumar, V.; Johnson, S. P.; Richardson, S.; Goncalves, M.; Parkes, H. G.; Arstad, E.; Thomas, D. L.; Pedley, R. B.; Lythgoe, M. F.; Golay, X. *Nat. Med.* **2013**, *19*, 1067.
(14) van Zijl, P. C. M.; Jones, C. K.; Ren, J.; Malloy, C. R.; Sherry, A. D. *Proc. Natl. Acad. Sci. U. S. A.* **2007**, *104*, 4359.
(15) Ling, W.; Regatte, R. R.; Navon, G.; Jerschow, A. *Proc. Natl. Acad. Sci. U. S. A.* **2008**, *105*, 2266.
(16) Zhou, J. Y.; Wilson, D. A.; Sun, P. Z.; Klaus, J. A.; van Zijl, P. C. M. *Magn. Reson. Med.* **2004**, *51*, 945.
(17) Sun, P. Z.; Zhou, J. Y.; Sun, W. Y.; Huang, J.; van Zijl, P. C. M. *J. Cereb. Blood Flow Metab.* **2007**, *27*, 1129.
(18) Long, D.; Marshall, C. B.; Bouvignies, G.; Mazhab-Jafari, M. T.; Smith, M. J.; Ikura, M.; Kay, L. E. *Angew. Chem., Int. Ed.* **2013**, *52*, 10771.
(19) Bouvignies, G.; Kay, L. E. *J. Biomol. NMR* **2012**, *53*, 303.
(20) Xu, J.; Yadav, N. N.; Bar-Shir, A.; Jones, C. K.; Chan, K. W.; Zhang, J.; Walczak, P.; McMahon, M. T.; van Zijl, P. C. *Magn. Reson. Med.* **2014**, *71*, 1798.
(21) Xu, X.; Yadav, N. N.; Zeng, H. F.; Jones, C. K.; Zhou, J. Y.; van Zijl, P. C. M.; Xu, J. D. *Magn. Reson. Med.* **2016**, *75*, 88.
(22) Bai, Y. W.; Milne, J. S.; Mayne, L.; Englander, S. W. *Proteins: Struct., Funct., Genet.* **1993**, *17*, 75.
(23) McMahon, M. T.; Gilad, A. A.; DeLiso, M. A.; Berman, S. D. C.; Bulte, J. W. M.; van Zijl, P. C. M. *Magn. Reson. Med.* **2008**, *60*, 803.
(24) Garbow, J. R.; Weitekamp, D. P.; Pines, A. *Chem. Phys. Lett.* **1982**, *93*, 504.
(25) Friedman, J. I.; McMahon, M. T.; Stivers, J. T.; Van Zijl, P. C. M. *J. Am. Chem. Soc.* **2010**, *132*, 1813.
(26) Yadav, N. N.; Jones, C. K.; Xu, J. D.; Bar-Shir, A.; Gilad, A. A.; McMahon, M. T.; van Zijl, P. C. M. *Magn. Reson. Med.* **2012**, *68*, 1048.
(27) Marchal, J. P.; Canet, D. *Org. Magn. Reson.* **1981**, *15*, 344.
(28) Ardenkjaer-Larsen, J. H.; Fridlund, B.; Gram, A.; Hansson, G.; Hansson, L.; Lerche, M. H.; Servin, R.; Thaning, M.; Golman, K. *Proc. Natl. Acad. Sci. U. S. A.* **2003**, *100*, 10158.
(29) Nelson, S. J.; Kurhanewicz, J.; Vigneron, D. B.; Larson, P. E. Z.; Harzstark, A. L.; Ferrone, M.; van Criekinge, M.; Chang, J. W.; Bok, R.; Park, I.; Reed, G.; Carvajal, L.; Small, E. J.; Munster, P.; Weinberg, V. K.; Ardenkjaer-Larsen, J. H.; Chen, A. P.; Hurd, R. E.; Odegardstuen, L. I.; Robb, F. J.; Tropp, J.; Murray, J. A. *Sci. Transl. Med.* **2013**, *5*, 198ra108.
(30) Kurhanewicz, J.; Vigneron, D. B.; Brindle, K.; Chekmenev, E. Y.; Comment, A.; Cunningham, C. H.; DeBerardinis, R. J.; Green, G. G.; Leach, M. O.; Rajan, S. S.; Rizi, R. R.; Ross, B. D.; Warren, W. S.; Malloy, C. R. *Neoplasia* **2011**, *13*, 81.

DOI: 10.1021/jacs.6b06421
J. Am. Chem. Soc. 2016, 138, 11136−11139